

# The Impact of Stroma Admixture on Molecular Subtypes and Prognostic Gene Signatures in Serous Ovarian Cancer

Matthew Schwede<sup>1</sup>, Levi Waldron<sup>2</sup>, Samuel C. Mok<sup>3</sup>, Wei Wei<sup>4</sup>, Azfar Basunia<sup>1,5</sup>, Melissa A. Merritt<sup>6</sup>, Constantine S. Mitsiades<sup>7</sup>, Giovanni Parmigiani<sup>1,5</sup>, David P. Harrington<sup>1,5</sup>, John Quackenbush<sup>5</sup>, Michael J. Birrer<sup>8</sup>, and Aedin C. Culhane<sup>1,5</sup>



## ABSTRACT

**Background:** Recent efforts to improve outcomes for high-grade serous ovarian cancer, a leading cause of cancer death in women, have focused on identifying molecular subtypes and prognostic gene signatures, but existing subtypes have poor cross-study robustness. We tested the contribution of cell admixture in published ovarian cancer molecular subtypes and prognostic gene signatures.

**Methods:** Gene signatures of tumor and stroma were developed using paired microdissected tissue from two independent studies. Stromal genes were investigated in two molecular subtype classifications and 61 published gene signatures. Prognostic performance of gene signatures of stromal admixture was evaluated in 2,527 ovarian tumors (16 studies). Computational simulations of increasing stromal cell proportion were performed by mixing gene-expression profiles of paired microdissected ovarian tumor and stroma.

**Results:** Recently described ovarian cancer molecular subtypes are strongly associated with the cell admixture. Tumors were classified as different molecular subtypes in simulations where the percentage of stromal cells increased. Stromal gene expression in bulk tumors was associated with overall survival (hazard ratio, 1.17; 95% confidence interval, 1.11–1.23), and in one data set, increased stroma was associated with anatomic sampling location. Five published prognostic gene signatures were no longer prognostic in a multivariate model that adjusted for stromal content.

**Conclusions:** Cell admixture affects the interpretation and reproduction of ovarian cancer molecular subtypes and gene signatures derived from bulk tissue. Elucidating the role of stroma in the tumor microenvironment and in prognosis is important.

**Impact:** Single-cell analyses may be required to refine the molecular subtypes of high-grade serous ovarian cancer.

## Introduction

There have been several attempts to identify molecular subtypes and prognostic genomic signatures for advanced-stage serous ovarian cancers (1–4). The first large study to report molecular subtypes studied mostly serous tumors and identified a subtype that was associated with poor overall survival, C1 (1). Subsequently, The Cancer Genome Atlas (TCGA) study reported four similar subtypes in high-grade serous ovarian cancer (HGSOC) but found no difference in clinical outcome between the subtypes (2), which led researchers to question the clinical utility of these classifications (5). Subtype pre-

dictions using the TCGA classification are not consistently robust, sometimes producing overlapping clusters, with most tumors assigned to more than one subtype (6, 7). A recent comprehensive meta-analysis could not robustly classify subtypes across data sets (8), leading to alternative subtype classifications that were associated with survival, tumor purity, age, and lymphocyte infiltration (8).

Molecular subtype and biomarker discovery in HGSOC has mostly been performed on gene-expression profiles of bulk tumors that may include fibroblasts, immune cells, and endothelial cells (9). The gene-expression profile of a bulk tumor is the mean of the admixture of malignant epithelial, stromal, and other cells, but gene-expression studies of bulk tumors rarely record or adjust for tumor purity, which can be highly variable within and between studies. Stromal content is variable in two of the largest gene-expression profiling studies (1, 2). In the Australian Ovarian Cancer Study (AOCS), 40% of tumors in the molecular subtype C1 had low tumor percentage ( $\leq 50\%$ ) compared with 9% in the other molecular subtypes combined (1). In the TCGA study, the proportion of stromal cells exceeded 50% in about 1% of tumors, and the median proportion of stromal cells was 10% (2).

The relative proportions of tumor and stromal cells may also be an independent prognostic indicator in several epithelial cancers, including breast (10), colon (11), and possibly ovarian cancer (12). Cells in the tumor microenvironment are important for chemosensitivity (13), and genes expressed by cells in the tumor microenvironment are prognostic in ovarian cancer (4, 14–16). For example, activation of Smad signaling in cancer-associated fibroblasts in the tumor microenvironment is associated poor patient survival (16).

Additionally, cancer type – or subtype-specific biomarkers obtained in bulk gene-expression profiling studies may include genes expressed by stromal or immune cells. Recent studies report discovery of six immune subtypes in 33 cancer types (17) and two stromal subtypes in ovarian cancer (16). The potentially complex relationships between nonmalignant cells in the HGSOC tumor microenvironment and

<sup>1</sup>Department of Data Sciences, Dana-Farber Cancer Institute, Boston, Massachusetts. <sup>2</sup>Biostatistics, CUNY Graduate School of Public Health and Health Policy, New York, New York. <sup>3</sup>Department of Gynecologic Oncology and Reproductive Medicine, The University of Texas MD Anderson Cancer Center, Houston, Texas. <sup>4</sup>Pfizer, Andover, Massachusetts. <sup>5</sup>Department of Biostatistics, Harvard T.H. Chan School of Public Health, Boston, Massachusetts. <sup>6</sup>University of Hawai'i Cancer Center, Honolulu, Hawai'i. <sup>7</sup>Department of Medical Oncology, Dana-Farber Cancer Institute, Boston, Massachusetts. <sup>8</sup>Division of Hematology-Oncology, University of Alabama at Birmingham, Birmingham, Alabama.

**Note:** Supplementary data for this article are available at Cancer Epidemiology, Biomarkers & Prevention Online (<http://cebp.aacrjournals.org/>).

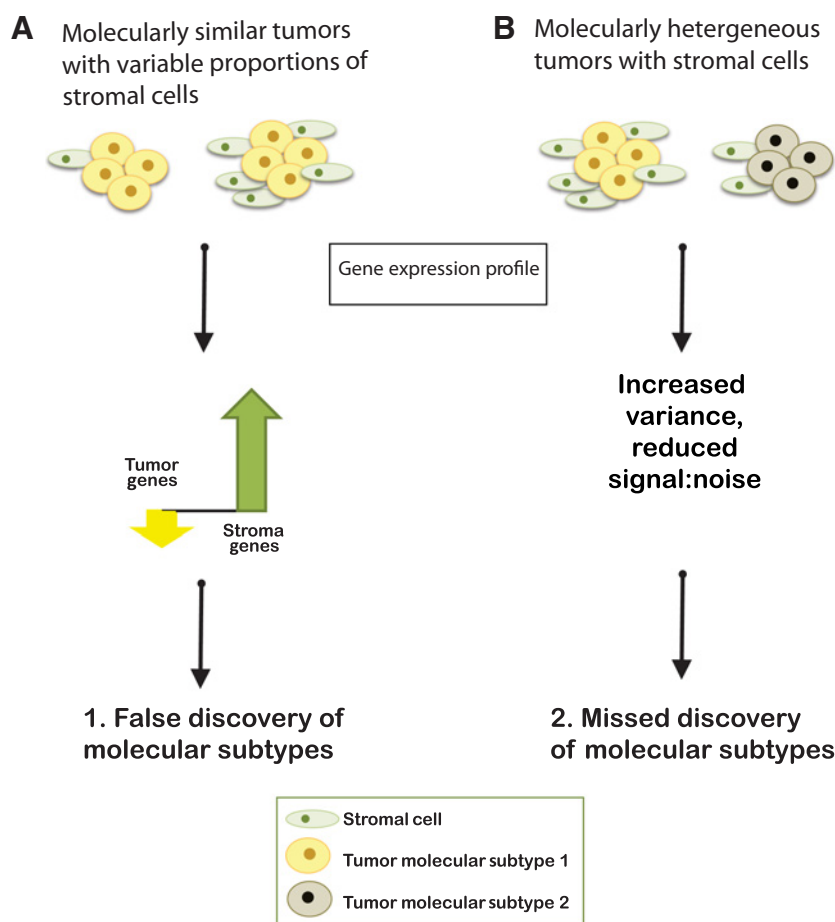
Current address for M.J. Birrer: Winthrop P. Rockefeller Cancer Institute, Little Rock, Arkansas.

**Corresponding Authors:** Aedin C. Culhane, Dana-Farber Cancer Institute, Harvard T.H. Chan School of Public Health, 450 Brookline Avenue, LC9323, Boston, MA 02115. Phone: 617-632-2468; E-mail: [aein@jimmy.harvard.edu](mailto:aein@jimmy.harvard.edu); and Michael J. Birrer, Winthrop P. Rockefeller Cancer Institute, 4301 W. Markham Street, Little Rock, AR 72205. Phone: 501-526-2272; E-mail: [Mjbirrer@uams.edu](mailto:Mjbirrer@uams.edu)

Cancer Epidemiol Biomarkers Prev 2020;29:509–19

doi: 10.1158/1055-9965.EPI-18-1359

©2019 American Association for Cancer Research.

**Figure 1.**

Variability in stromal proportions may present challenges in gene expression analysis of bulk tissue. **A**, If two tumors of the same molecular subtype have different proportions of stromal cells, the observed average gene expression in the tumor with more stromal cells will show an increase in stroma-associated gene expression with a concurrent decrease in tumor-associated gene expression. This apparent decrease in tumor gene expression may result in false discovery of molecular subtypes. **B**, Different proportions of stromal cells will increase noise in analysis, which may cause researchers not to discover underlying molecular subtypes.

malignant epithelial cell gene expression are unknown, but sampling variability in the cell admixture may affect subtype discovery (**Fig. 1**). Single-cell gene-expression profiling may resolve many of these issues, but the extent to which nonmalignant cell admixture has influenced the field to date is unknown.

We systematically explored the extent to which stromal cell admixture in tumor samples influences molecular subtype and prognostic gene signature discovery (**Fig. 1**). We hypothesized that, if unadjusted in statistical analyses, variance in the percent of stromal cells may lead to false discovery of tumor molecular subtypes, low precision of tumor classification, and reduced power to detect true ovarian epithelial carcinoma molecular subtypes and prognostic signatures. We tested this by identifying genes that were differentially expressed between microdissected tumor and stromal cells and examining whether these genes were enriched in published serous ovarian cancer subtypes and prognostic gene-expression signatures. We show that stromal gene expression and gene signatures of stromal cell admixture are associated with overall survival in a meta-analysis of HGSOc gene expression data sets. We also investigate the number of published prognostic ovarian cancer gene signatures that add prognostic information to tumor–stroma proportion.

## Materials and Methods

### Data

Details and sources of all data sets are listed in Supplementary Table S1. Raw gene-expression data for two AOCS data sets (2) were

downloaded from Gene-Expression Omnibus (GEO). These AOCS data sets were (i) high-grade (G2 and G3) ovarian adenocarcinomas ( $n = 215$ ; 11 endometrioid, 203 serous and 1 undifferentiated) that were previously classified as high-grade molecular subtypes C1, C2, C4, or C5 (the “AOCS data set,” GEO GSE9891) and (ii) a subset of four C1 tumors that had matched microdissected tumor and stroma (the “AOCS microdissected dataset,”  $n = 8$ , GEO GSE9890). We excluded low-grade and low malignant potential AOCS subtypes (C3 and C6 subtypes,  $n = 36$ ) and unclassified tumors ( $n = 34$ ). The Massachusetts General Hospital (MGH) ovarian cancer data set was received directly from the authors and included Affymetrix gene-expression profiles of pairs ( $n = 38$ ) of microdissected tumor and stroma of HGSOc from women hospitalized at the MGH (GSE18520 and GSE40595, the “MGH dataset”; refs. 18, 19). The MGH data set also included unmatched normal ovary stroma ( $n = 10$ ). In TCGA ovarian cancer data set ( $n = 518$ , downloaded November 24, 2010), all but one tumor was high-grade serous (2). Public gene-expression data from 16 studies were extracted from the curatedOvarianData (20) database. Nonovarian validation data sets were downloaded from GEO (Supplementary Table S1) and included microarray gene-expression profiles of microdissected stroma and tumor from noninflammatory breast cancer ( $n = 34$  pairs; GSE5847, Boersma and colleagues, ref. 21) and invasive breast cancer ( $n = 28$  pairs; GSE10797, Casey and colleagues, ref. 22). These also included two prostate cancer data sets with known percent stromal content (GSE17951,  $n = 136$ ; GSE8218,  $n = 109$ ; ref. 9).

To compare bulk and microdissected AOCS molecular profiles, raw data (cel files) were normalized using frozen robust multiarray analysis (fRMA; ref. 23), which uses an external reference normalization approach, allowing one to combine data from different batches (when these data were generated using the same platform). Other GEO raw data sets were normalized using RMA (24, 25). Data in curated OvarianData were used as provided because these have been extensively manually curated, uniformly preprocessed, and normalized.

### Statistical analysis

Analyses were performed using R and Bioconductor, versions 2.15 and 2.10, respectively, or later.

### Gene signatures of tumor and stroma

Genome-wide differential gene-expression analyses were performed using a moderated  $t$  test, and  $P$  values were adjusted for multiple testing using the Benjamini–Hochberg method (26) from the Bioconductor package limma (27). For paired microdissected stroma and tumor samples, a paired moderated  $t$  test with a  $P$  value cutoff of 0.01 was used. A separate analysis of the AOCS microdissected data set with a less stringent cutoff ( $P < 0.05$ ) was also performed to identify a broader set of tumor and stromal genes. Genes that were differentially expressed between each AOCS or TCGA molecular subtypes were detected using an unpaired test. In differential gene-expression analysis of the MGH data set, a more stringent  $P$  value cutoff was applied to generate gene lists of similar length. Hierarchical clustering was performed using Pearson correlation with average linkage clustering (28).

Tissue-specific tumor or stroma marker genes were identified by transforming gene expression to binary on/off calls (29) and ranking genes that were expressed in one tissue and not expressed in the other microdissected tissues. Genes were considered tissue-specific if they had high sensitivity and specificity (area under a receiver operating curve  $\geq 0.9$ ).

To generate a single gene signature covariate in statistical models, a gene signature score was computed using a weighted sum approach as previously described (30). Positive weights (+1) were applied to genes upregulated in poor-prognosis tumors, BRCA mutation-like tumors, metastases, an angiogenic subtype, or malignant tumors. Negative weights (−1) were applied to the other genes in the signature. Linear regression was used to test for association between continuous variables and percent stromal content. Fisher exact test was used to test for overlap between gene sets, with the background number of genes equal to the number of probes or genes on the platform (e.g., the AOCS  $n = 18,769$ ).

### Molecular subtype prediction

The gene lists reported to predict AOCS and TCGA molecular subtypes were downloaded as online publication supplements (1, 2), curated, and submitted to GeneSigDB (31). To reproduce the AOCS and TCGA molecular subtype classifiers, gene lists were used to build subtype classifiers using the single sample predictor (SSP) approach (32). The centroids of gene-expression profiles of the four molecular subtypes in the AOCS study (C1, C2, C4, and C5; ref. 1) and TCGA study (mesenchymal, immunoreactive, differentiated, proliferative; ref. 2) were calculated (Supplementary Fig. S1), and cases (tumor or stroma) were assigned to the molecular subtype with highest Pearson correlation coefficient. A case was not classified to any molecular subtype (“unclassified”) if its correlation to each one of the subtypes was less than 0.7. There was high concordance in classification between our implementation of the subtype classifiers

and their original studies. The AOCS SSP molecular subtype classifier had a self-validation accuracy of 95%, sensitivity 0.93–0.97, and specificity 0.96–1.0 (Supplementary Fig. S1C). The TCGA molecular subtype SSP classifier had an overall self-validation accuracy of 89%, 0.84–0.94 sensitivity, and 0.95–0.98 specificity for each subtype (Supplementary Fig. S1D).

### Computational mixing of tumor and stroma fractions

Paired microdissected tumor and stroma ( $n = 38$ ) were computationally mixed in increasing increments of 10%, as described previously (33). The gene-expression values of each tumor ( $G_t$ ) were mixed with gene-expression values of its adjacent stroma ( $G_s$ ) using the linear combinations  $mG_t + (1 - m)G_s$ . Mixing parameter  $m$  is the proportion of tumor and  $1 - m$  is the proportion of stroma, incremented by 0.1 from 0 to 1. This was performed for all genes in the molecular subtype classifier to produce a computationally simulated mixture of tumor and stroma. The assumption of linearity has been previously supported by comparing the computational values to those observed in gene expression of cocultured cells for the breast molecular subtype PAM50 gene signature (33).

### Survival analysis

Cox proportional hazards regression was used to test for association between continuous variables and survival variables [relapse-free survival, overall survival (OS)]. In survival analyses of gene signatures using independent data sets, the  $P$  values were not corrected for multiple testing. Meta-analysis of the tumor–stroma gene signatures was performed using the metafor R package and summary hazard ratios and confidence intervals of the 16 studies ( $n = 2,527$  ovarian tumors) were calculated with a fixed-effects model.

### Exploratory data analysis of stromal genes and TCGA immune landscape signatures

Additional clinical data, stromal fraction, leukocyte fraction, five core immune signatures (wound-healing, macrophage regulation, lymphocyte infiltration, interferon gamma response, and TGF $\beta$  response), CIBERSORT estimates of >25 immune cell types, and mutation load for each TCGA HGSOC tumor were downloaded from the TCGA immune landscape study (17) article supplement (<https://isb-cgc.shinyapps.io/shiny-iatlas/>). The Spearman rank correlation coefficient was used to summarize the relationship between stromal gene-expression score and immune features in TCGA HGSOC tumors.

## Results

We investigated the extent to which non-tumor cell gene expression distinguishes HGSOC molecular subtypes using three different approaches: (i) cluster analysis to explore correlations between gene-expression profiles of microdissected tumor, microdissected stroma, and HGSOC tumors of different molecular subtypes, (ii) differential gene-expression analysis to determine if genes that are differentially expressed between molecular subtypes are also differentially expressed in microdissected tumor or stroma, and (iii) *in silico* cell admixture analysis to discover the robustness of molecular subtype classifications to increasing proportion of stromal cells.

### Defining HGSOC tumor and stroma gene signatures

We defined gene-expression signatures that characterize HGSOC and its adjacent stroma using paired laser microdissected tissue from two independent studies. Using the AOCS microdissected data set, we

defined a 688-gene signature using C1/stromal tumors ( $n = 8$ ;  $P < 0.01$ , paired  $t$  test with modified variance (27) and FDR correction (ref. 26; Supplementary Table S2). This AOCs tumor–stroma gene signature contained 461 and 227 unique genes with increased expression in C1 stroma and tumor, respectively, which are referred to as the “stromal gene set” and “tumor gene set.” A list with a larger number of genes extracted using lower differential expression stringency ( $P < 0.05$ ) is available in Supplementary Table S2. In a second, independent analysis of paired microdissected tumor and stroma from HGSOC tumors of 38 patients in an MGH study (18), we identified a similar gene signature. This MGH tumor–stroma gene signature of 519 unique genes contained 429 and 90 genes that had higher expression in stroma and tumor, respectively (Supplementary Table S2). Despite the small sample size from which the AOCs tumor–stroma signature was derived, the MGH signature had significant overlap with it: 24/90 genes overexpressed in tumor (Fisher exact test  $P < 10^{-10}$ ) and 122/429 genes overexpressed in stroma ( $P < 10^{-25}$ ). The concordance of these signatures was supported by the observation that the AOCs signature correctly discriminated all but one of the microdissected tumor and stroma MGH specimens using unsupervised hierarchical cluster analysis (Supplementary Fig. S2).

#### Cluster analysis of microdissected tumor, stroma, and their bulk gene-expression profiles

Using these tumor–stroma gene signatures, we investigated the contribution of stromal cell gene expression to the HGSOC molecular subtype using unsupervised cluster analysis. The 688-gene AOCs tumor–stroma gene signature partitioned the AOCs high-grade serous tumors ( $n = 215$ ) into two clusters (Fig. 2): those with low versus high stromal gene expression. These two clusters could be further subdivided to form four clusters, which largely reflected the four AOCs HGSOC molecular subtypes: C4/CA125, C5/MYC deregulation (34), C2/immunoreactive, and C1/stromal. We observed that matched microdissected tumor samples did not cluster with the corresponding bulk tumor. Instead, microdissected C1 tumors clustered with C4/CA125 molecular subtype tumors, whereas microdissected C1 stroma clustered with the C1 bulk tumors.

The MGH tumor–stroma gene signature similarly partitioned the AOCs data set into clusters (Supplementary Fig. S2C) which reflected AOCs HGSOC molecular subtypes, particularly the split of C1 compared with others. The observation that C1 tumors had higher stromal content is known, but the high concordance of tumor and stroma clusters with published HGSOC molecular subtypes suggested that genes that are differentially expressed between tumor and stroma might be sufficient to discriminate the HGSOC molecular subtypes.

#### Stromal genes are differentially expressed between ovarian cancer molecular subtypes

These molecular subtypes were then further examined using gene-expression analysis, in which we quantified the relative contribution of stroma and tumor gene expression to each molecular subtype. We performed global differential gene expression analysis between each pair of AOCs tumor molecular subtypes [C1, C2, C4, and C5; limma (ref. 27), 2-fold change and  $P < 0.001$  after FDR correction; Supplementary Table S3A]. The number of genes that discriminated between each pair of subtypes varied in size from 343 (C1 vs. C2) to 1,267 (C1 vs. C5; Fig. 3A). We tested the overlap between these gene lists and the AOCs stromal and tumor gene sets. The stromal and tumor gene sets derived from the AOCs microdissected data set's C1 tumors were again used so that the gene sets were most comparable. We observed that any contrast involving C1 had strong overlap with the stromal

gene set (Fisher test  $P < 10^{-61}$ ), as did the contrast of C2 versus C4 (Fisher test  $P < 10^{-73}$ ). Specifically, 54% and 41% of genes significantly different in contrasts of C1 versus C2 or C1 versus C4, respectively, were upregulated in stromal cells (Fig. 3A). This suggests that at least C1 is primarily driven by different amounts of stromal gene expression. In contrast, only 9% of genes differentially expressed between C4 and C5 were stromal genes ( $P = 1$ ), consistent with the subtypes' reported low amount of desmoplasia (1). The tumor gene set and “other” genes dominated C5 differential gene expression, consistent with C5's distinct molecular properties (2, 34).

Based on these results, we also investigated the influence of stromal gene expression in TCGA HGSOC molecular subtypes (Fig. 3B; Supplementary Table S3B). The TCGA mesenchymal, immunoreactive, differentiated, and proliferative subtypes have highest global gene-expression correlation with the AOCs subtypes C1, C2, C4, and C5, respectively (Fig. 3C), and the mesenchymal subtype has significantly higher percent stromal content than other subtypes ( $t$  test  $P = 1.35 \times 10^{-7}$ ). Results from analysis of the TCGA study confirmed findings in the AOCs subtype analysis. Genes differentially expressed ( $P < 0.001$ , FDR correction) in the TCGA mesenchymal subtype, similar to C1, were mostly in the stromal gene set (Fig. 3D, 59%), and overlapped strongly (35%) with genes differentially expressed in C1 (Fig. 3D). Similar to the AOCs C4 and C5 subtypes, few genes in the stromal gene set were differentially expressed between TCGA's differentiated and proliferative molecular subtypes ( $<5\%$ ,  $P = 1$ ). Lastly, genes that were differentially expressed in the proliferative subtype, similar to C5, were relatively enriched in tumor-specific and “other” genes.

Similar results were observed when these analyses were repeated with the MGH tumor and stroma signatures (Supplementary Table S3C). Similar to the AOCs tumor signature, the MGH tumor signature did not significantly overlap with gene lists from pairwise comparisons of any two AOCs or TCGA molecular subtypes ( $P = 1$  for overlap with any comparison). Consistent with the AOCs stromal signature, the MGH stromal signature strongly overlapped with comparisons between the AOCs C1 subtype and either C2 or C4 and similar comparisons between the TCGA mesenchymal subtype and either the immune or differentiated subtypes. We observed that 24% and 19% of genes differentially expressed between C1 versus C2 ( $P < 10^{-13}$ ) and C1 vs. C4 ( $P < 10^{-15}$ ), respectively, were MGH stromal genes. There was no significant overlap between MGH stromal genes and any pairwise comparison involving the AOCs C5 subtype ( $P = 1$ ). Therefore, in two independent studies, stroma-associated expression explains a large portion of the differential gene expression of select subtypes.

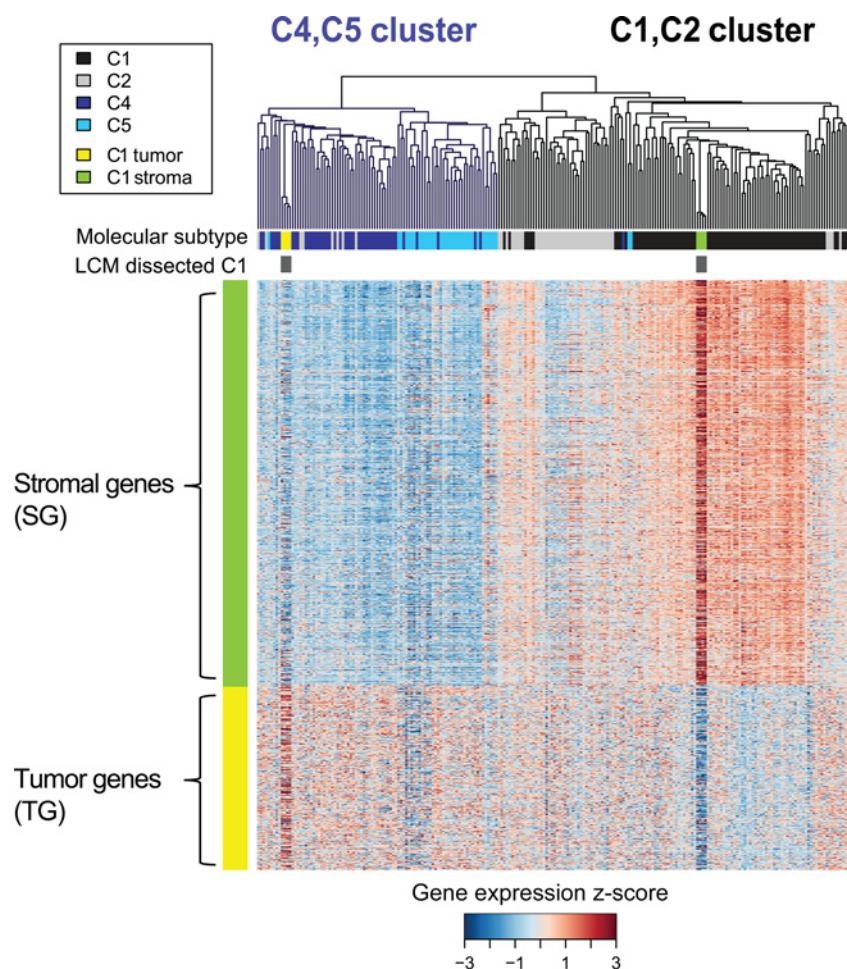
#### Molecular subtype classifications change with the proportion of stromal gene expression

We next investigated if the gene signature classifiers for these molecular subtypes were stable when the proportion of stromal cells changed. We trained an SSP classifier using the gene lists reported to predict each of the AOCs C1, C2, C4, and C5 molecular subtypes (ref. 1; Supplementary Fig. S1A and S1C). When applying the AOCs classifier to epithelial carcinoma cells microdissected from HGSOC tumors in an independent cohort (MGH data set  $n = 38$ ), most microdissected tumors (20/38) were assigned to subtype C4 (Supplementary Fig. S1E and S1I). Matched microdissected stroma was all classified as C1 ( $n = 23$ ) or unclassified ( $n = 15$ ; Supplementary Fig. S1G and S1J). However, computational mixing of only 10% stromal gene expression with paired microdissected tumor caused 6/38 tumors to be reclassified (Supplementary Fig. S3A), including C4



**Figure 2.**

AOCS molecular subtypes can be distinguished by stromal and tumor gene expression. Analysis of gene-expression profiles of microdissected epithelial tumor cells and stroma from four C1 tumors identified a 688-gene ovarian tumor–stroma gene signature (FDR-adjusted  $P < 0.01$ ). The signature contained 461 genes that were overexpressed in microdissected stroma and 227 genes with increased expression in epithelial tumor cells, and these distinguished ovarian tumor and stroma in an independent MGH data set (Supplementary Fig. S2). The heatmap shows the tumor and stromal gene-expression profiles in the AOCS's HGSOC tumors and microdissected C1 stroma and tumor samples. C1 microdissected stroma samples clustered with C1 subtype tumors, whereas the C1 microdissected tumor samples clustered with C4 subtype tumors. All of these analyses were done using unsupervised hierarchical cluster analysis. Colors of the heatmap were scaled (z-score values across rows).



tumors that were reclassified as C1 ( $n = 2$ ) or C2 ( $n = 2$ ). Molecular subtype C5 tumors remained stable, reflecting the lack of stromal gene expression determining this subtype. Five additional tumors were predicted to have a different molecular subtype when the stromal content was increased to 20%, and at 30% stroma, over one third (15/38) of tumors' subtypes were reassigned.

We observed similar results regarding the robustness of TCGA molecular subtypes with increasing proportions of stroma. We built an SSP classifier of TCGA molecular subtypes using their 100-gene signature (ref. 7; Supplementary Fig. S1B and S1D). When it was applied to classify microdissected tumors in the MGH data set, most were assigned either to the differentiated subtype (23/38), which is similar to the AOCS C4 subtype, or to the proliferative subtype (8/38), which is similar to C5 (Supplementary Fig. S1F and S1I). Microdissected stroma was classified as mesenchymal (20/38) or was unclassified (10/38; Supplementary Fig. S1H and S1J). With 10%, 20%, and 30% stroma, 0/38, 5/38, and 8/38 tumors, respectively, were classified to a different molecular subtype (Supplementary Fig. S3B). Thus, the percentage of stromal content influences subtype classification.

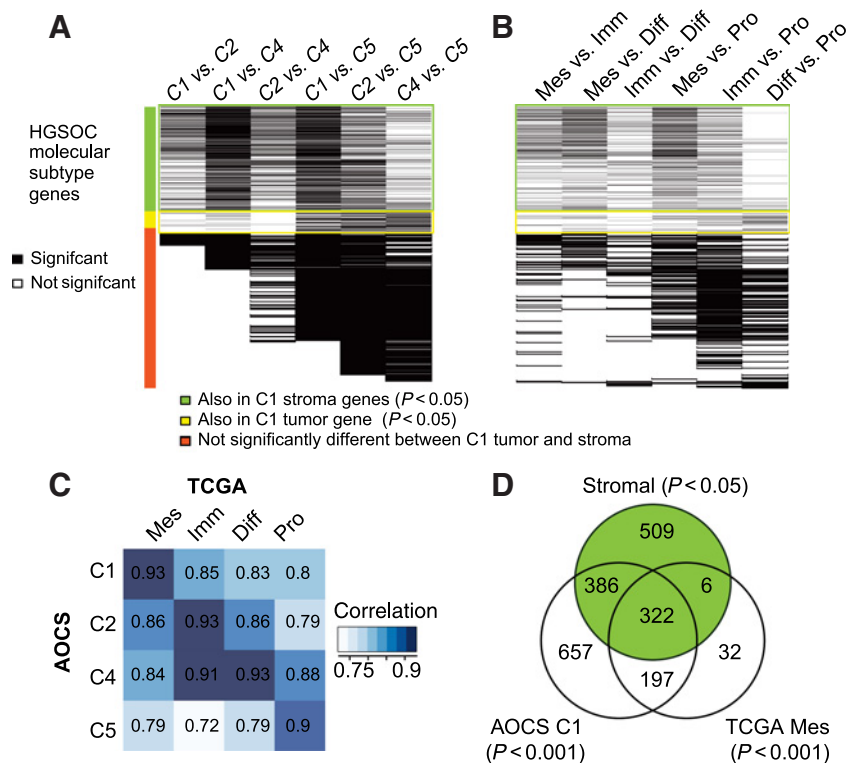
#### The association between the proportion of stroma in tumors and OS in HGSOC

The AOCS C1/stromal subtype is reported to have a worse prognosis, and therefore we explored whether percent stroma itself was prognostic. We confirmed that the AOCS C1/stromal subtype,

which has high stromal proportion, was associated with poorer OS. C1 had a hazard ratio (HR) of 1.72 (95% confidence interval 1.15–2.58,  $P = 0.0083$ ). The AOCS C1/stromal molecular subtype had a HR of 1.49 (95% CI, 0.99–2.26,  $P = 0.056$ ) within high stage (III or IV) tumors.

In the TCGA data, pathologist scores of percent stromal content had a weak but significant (HR 1.01 for each percent increase in stromal content, CI 1.0–1.02,  $P = 0.024$ ) association with OS in univariate Cox proportional hazards regression analyses of high stage tumors, but not across all tumors (HR 1.0, CI 0.99–1.02,  $P = 0.088$ ; Fig. 4C for survival association with stromal content > 30%). In other studies, no estimate of the percentage of stroma was available, but we assessed the prognostic power of a tumor–stroma gene signature in an aggregated cohort of 2,527 HGSOC patients from 16 studies, which included the TCGA and AOCS data sets (20). The 688-gene AOCS tumor–stroma signature had a HR of 1.17 (95% confidence interval 1.11–1.23; Fig. 4A).

The AOCS and MGH tumor–stroma signatures were generated using differential gene-expression analysis and might include genes that are expressed in both tumor and stroma cells, albeit at different levels. Therefore, we derived a list of markers specific to tumor or stroma that better reflect cell admixture. Using expression profiles of paired microdissected epithelial tumor (MGH data set  $n = 38$ ), adjacent tumor stroma ( $n = 38$ ), and unrelated normal ovarian stroma ( $n = 10$ ), we applied a barcode approach (29) to convert gene

**Figure 3.**

Overlap between genes that are differentially expressed between the AOCs and TCGA molecular subtypes and tumor-stroma gene sets. Black and white lines indicate genes that were or were not strongly differentially expressed (limma, moderated  $t$  statistics,  $P < 0.001$  after FDR correction), respectively, between each pair of AOCs (**A**) and TCGA (**B**) molecular subtypes. The color bar indicates whether these genes were also differentially expressed in laser capture microdissected C1 tumor (yellow) and stroma (green) at  $P < 0.05$ , or not significantly differentially expressed between C1 tumor and stroma (orange). Stromal and tumor genes with cutoff  $P < 0.05$  rather than 0.01 were used in order to explore the extent of stromal gene enrichment in these subtypes. **C**, Correlation between average expression of AOCs and TCGA molecular subtypes, which was calculated using the intersection of all differentially expressed genes between any pair of AOCs or TCGA subtypes. Mes, Imm, Diff, and Pro are the TCGA molecular subtypes: mesenchymal, immunoreactive, differentiated, and proliferative, respectively. **D**, There was a large overlap between genes expressed in C1 microdissected stroma and genes that were differentially expressed either between C1 versus other AOCs subtypes or between the TCGA mesenchymal subtype versus other TCGA subtypes.

expression to binary expressed or not expressed calls. We then extracted a list of 28, 11, and 38 tissue markers with high specificity (Supplementary Fig. S4) for tumor, stroma adjacent to tumor, or normal ovary stroma (Supplementary Table S2). The 11 cancer-associated stromal tissue markers had similar prognostic power (HR, 1.17; CI, 1.11–1.23; Fig. 4B), but the tumor markers were not prognostic (HR, 0.96; CI, 0.96–1.01) and performed comparably to a randomly selected 20-gene signature (HR, 0.96; CI, 0.96–1.02). These results support that a higher stroma proportion in HGSOC tumors is associated with worse OS.

### Some prognostic ovarian cancer signatures predict stroma proportion in HGSOC

Given that stromal gene expression was associated with survival in HGSOC tumors, we hypothesized that some published prognostic ovarian cancer gene signatures might incidentally be proxies for the presence of stromal tissue. Published gene signatures of ovarian cancer ( $n = 61$ ) were downloaded from the database GeneSigDB (31) or curated from the literature (Supplementary Table S4). Gene signatures varied in size from 4 to 1,903 genes, with a median of 47 genes. Most gene signatures, including the TCGA study's prognostic signature and Konstantinopoulos and colleagues BRCAness signature (35), were not significantly enriched in stromal genes (Supplementary Table S4) and not associated with percent stromal content in TCGA samples (Table 1).

Over a third of published prognostic gene signatures ( $n = 21/61$ ) were enriched in AOCs stromal genes, and 9/61 were enriched in MGH stroma genes ( $P < 0.05$  after FDR correction). Eight signatures were further analyzed (Table 1); seven had strong enrichment ( $P < 0.001$ ) in both the AOCs and MGH stromal genes (Supplementary Table S4), and the Biade and colleagues benign tumor signature (36) nearly met these  $P$  value cutoffs. All of these eight signatures (AOCs signatures; Biade and colleagues benign tumor signature, ref. 36;

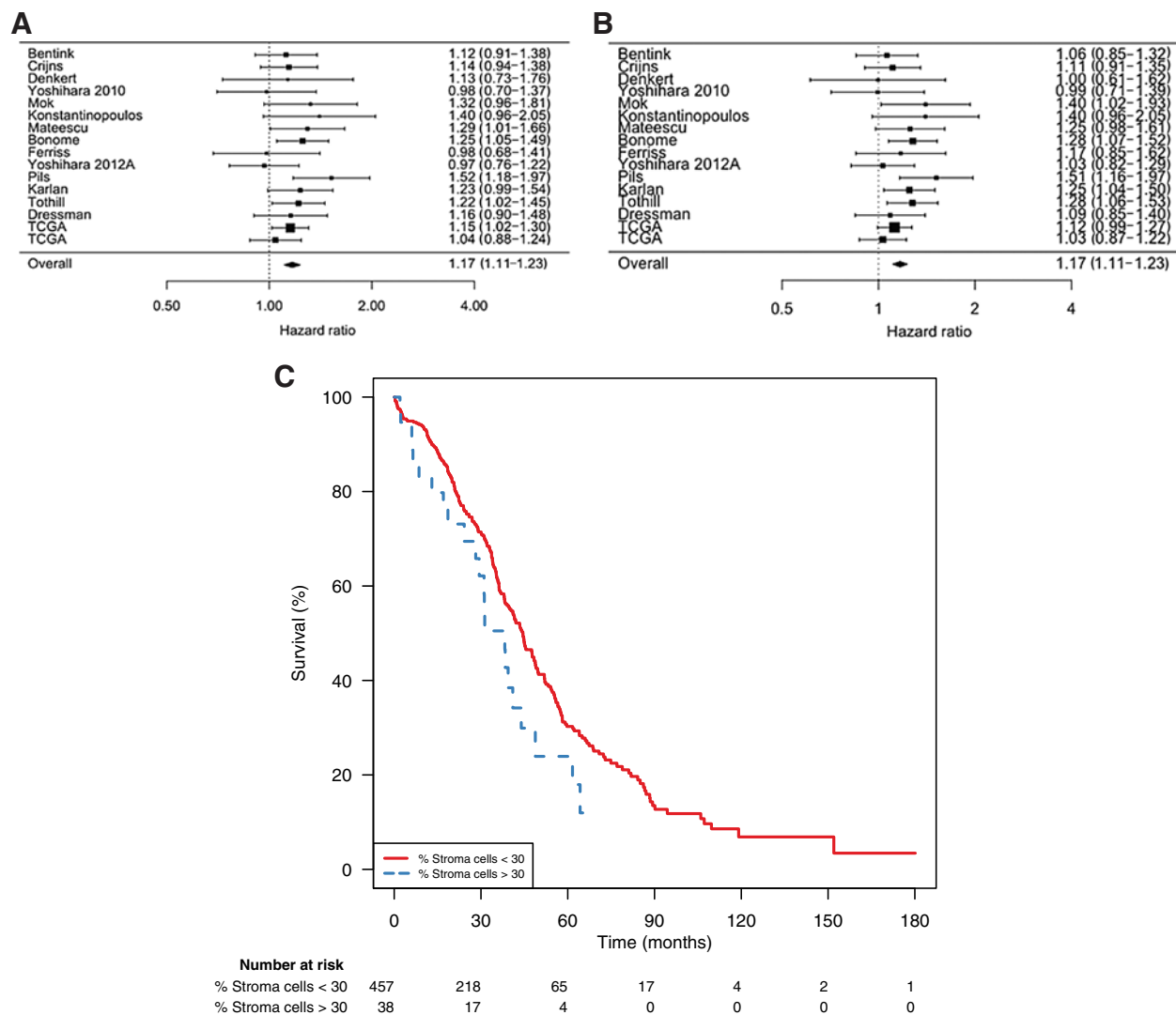
Bentink and colleagues, angiogenic signatures, ref. 14; and prognostic signatures from Bignotti and colleagues, ref. 37; Bonome and colleagues, ref. 38; and Spentzos and colleagues, ref. 39) were positively associated with pathologic scores of percent stromal content in TCGA tumors (linear regression,  $P < 10^{-8}$ ; Table 1B). Genes reported to be associated with poor prognosis overlapped with the stromal gene set in 7/8 gene signatures ( $P < 0.001$ ), whereas the good prognosis genes were often enriched in the tumor gene sets (Table 1A). The Biade and colleagues signature (36) was an exception, which had increased stromal cell proportions in benign tumor samples (36).

### Gene signatures enriched in stromal genes may provide little additional prognostic information beyond tumor-stroma ratio

Most of the eight gene signatures that were enriched in stromal genes were no longer associated with poor OS when adjusted for pathologist's estimates of percent stromal content in TCGA tumors in Cox proportional hazard regression analysis (Table 2A). The AOCs prognostic gene signatures remained associated with OS and progression-free survival (PFS) when adjusted for stromal content ( $P < 0.01$  and  $P < 0.05$ , respectively; Table 2A) but were no longer significant after adjusting for both stromal content and stage. Gene signatures not enriched in stromal genes, such as the BRCAness signature, remained associated with OS in multivariate models that adjusted for both stromal content and stage ( $P < 0.05$ ; Table 2A).

### The stromal signature is not specific to HGSOC

Several types of carcinoma cells have complex interactions with cells in the tumor microenvironment. Therefore, we asked whether stromal genes derived from ovarian cancer are specific to HGSOC or might more broadly characterize epithelial cancers. Each of the eight ovarian cancer signatures enriched in stromal genes were strongly associated with stroma versus epithelial components of breast cancer (Boersma and colleagues, ref. 21; Casey and colleagues, ref. 22) or percent stromal

**Figure 4.**

Stromal content's association with OS. These forest plots examine association with OS across ovarian cancer studies ( $n = 16$ ) using the AOCS tumor and stromal gene signatures (**A**) or only the genes that were specific to tumor-associated stroma from the MGH study (**B**). The two TCGA gene-expression data sets are  $n = 510$  Affymetrix HT\_HG-U133A and  $n = 256$  Illumina HiSeq RNA-seq. **C**, Kaplan-Meier curves of the pathologist assessment of percent stroma (cutoff of 30%) in high-stage TCGA tumors (HR 1.01 for each percent increase in stromal content, CI, 1.0–1.02;  $P = 0.024$ ). A 30% stroma threshold is shown because it is between the original TCGA consortium tumor purity threshold of at least 80% and the later reduced threshold of 60% tumor cells.

content in prostate cancer (Wang and colleagues, ref. 9; **Table 1**, linear regression or paired  $t$  test  $P < 10^{-4}$  in at least 3 of 4 data sets).

#### Clinical variables that explain stromal genes' association with survival

We observed that the strength of association between greater stromal proportion and survival was variable across data sets. We hypothesized that this could be related to sampling heterogeneity. In the AOCS C1 subtype, 63% of tumor samples were from extra-ovarian sites (most commonly peritoneum, as defined by the AOCS study), which often reflects a higher stage and thus worse prognosis, compared with 19% extra-ovarian sampling in other AOCS subtypes (1). In the TCGA data set, every tumor except for four were reported to be sampled at the ovary/pelvis (2). After adjusting for whether the sampling location was extra-ovarian, C1's association with OS (adjust-

ed  $P = 0.065$ ) was substantially attenuated. Thus, C1's prognostic power is partially related to sampling location, which may in turn reflect tumor stage.

## Discussion

We show that the proportion of stroma admixture in bulk tumors is a source of differential gene expression that affects molecular subtyping and prognostic gene signature discovery in HGSOc.

Although adjacent stromal cross-talk can affect nearby epithelial cells' gene-expression patterns (16), this is a distinct phenomenon from changes in observed gene expression caused by the admixture of stromal and other cells in bulk tumors (tumor purity). In bulk gene-expression profiling, the "observed" measure is an average of all cells in the admixture, which varies if the proportions of cell types change. We

**Table 1.** Associations between ovarian cancer gene signatures, stromal genes (SG), tumor genes (TG), and percent stromal content.

Study	Published gene signature	Signature components	Number of genes <sup>a</sup>	(A) Overlap with SGs and TGs		(B) % Stroma content <sup>b</sup>		(C) Breast stroma vs. epithelium <sup>b</sup>		(D) Prostate % stromal content <sup>b</sup>	
				# TGs (%)	# SGs (%)						
AOCS CI subtype stromal and tumor genes		Stromal genes	461	0	461	5.6 × 10 <sup>-13</sup>		4.3 × 10 <sup>-8</sup>	7.1 × 10 <sup>-8</sup>	1.5 × 10 <sup>-9</sup>	4.9 × 10 <sup>-17</sup>
		Tumor genes	227	227	0						
AOCS signatures (Tothill et al.)		Up in CI	287	0	<b>176 (61)<sup>c</sup></b>	3.8 × 10 <sup>-11</sup>		2.8 × 10 <sup>-8</sup>	5.1 × 10 <sup>-7</sup>	4.9 × 10 <sup>-8</sup>	1.1 × 10 <sup>-14</sup>
		Down in CI	147	2 (1)	2 (1)						
		Poor PFS	135	0	<b>103 (76)<sup>c</sup></b>	8.6 × 10 <sup>-13</sup>		4.0 × 10 <sup>-9</sup>	4.1 × 10 <sup>-8</sup>	1.2 × 10 <sup>-9</sup>	2.0 × 10 <sup>-17</sup>
		Good PFS	143	<b>16 (11)<sup>c</sup></b>	0			4.6 × 10 <sup>-9</sup>	9.7 × 10 <sup>-8</sup>	1.7 × 10 <sup>-5</sup>	6.5 × 10 <sup>-13</sup>
		Poor OS	147	0	<b>101 (69)<sup>c</sup></b>	5.3 × 10 <sup>-11</sup>		1.6 × 10 <sup>-5</sup>	2.2 × 10 <sup>-8</sup>	1.6 × 10 <sup>-11</sup>	3.6 × 10 <sup>-17</sup>
MGH stroma vs. tumor signature		Good OS	146	<b>23 (16)<sup>c</sup></b>	0						
		Tumor-associated stroma	431	0	<b>125 (29%)<sup>c</sup></b>	6.5 × 10 <sup>-15</sup>					
MGH tissue-specific genes		Tumor	81	<b>23 (28%)<sup>c</sup></b>	0			8.1 × 10 <sup>-5</sup>	0.04	1.6 × 10 <sup>-6</sup>	1.0 × 10 <sup>-7</sup>
		Tumor-associated stroma	11	0	<b>5 (42%)<sup>c</sup></b>	2.1 × 10 <sup>-14</sup>		0.001 (-)	1.8 × 10 <sup>-8</sup> (-)	3.7 × 10 <sup>-9</sup> (-)	1.2 × 10 <sup>-19</sup> (-)
		Tumor	28	<b>17 (57%)<sup>c</sup></b>	0	0.136		1.5 × 10 <sup>-7</sup>	0.93	1.1 × 10 <sup>-6</sup>	6.8 × 10 <sup>-14</sup>
Bentink et al.		Angiogenic	74	0	<b>35 (47)<sup>c</sup></b>	1.6 × 10 <sup>-9</sup>					
		Nonangiogenic	19	0	1 (5)						
Bignotti et al.		Up in metastasis	89	0	<b>54 (61)<sup>c</sup></b>	1.2 × 10 <sup>-9</sup>		4.5 × 10 <sup>-7</sup>	5.2 × 10 <sup>-5</sup>	7.2 × 10 <sup>-4</sup>	7.2 × 10 <sup>-8</sup>
		Up in primary tumor	36	1 (3)	0						
Spentzos et al.		Unfavorable prognosis	73	0	<b>19 (26)<sup>c</sup></b>	1.7 × 10 <sup>-10</sup>		1.8 × 10 <sup>-5</sup>	0.0074 (-)	4.1 × 10 <sup>-14</sup>	1.0 × 10 <sup>-7</sup>
		Favorable prognosis	43	<b>4 (9)<sup>c</sup></b>	0						
Bonome et al.		Poor prognosis	288	0	<b>37 (13)<sup>c</sup></b>	9.4 × 10 <sup>-11</sup>		3.5 × 10 <sup>-6</sup>	1.5 × 10 <sup>-6</sup>	7.7 × 10 <sup>-5</sup>	3.0 × 10 <sup>-11</sup>
		Good prognosis	272	5 (2)	1						
Biade et al.		Malignant cluster	21	<b>4 (27)<sup>c</sup></b>	0	1.1 × 10 <sup>-12</sup> (-)		9.8 × 10 <sup>-8</sup> (-)	5.2 × 10 <sup>-6</sup> (-)	6.5 × 10 <sup>-10</sup> (-)	7.1 × 10 <sup>-13</sup> (-)
		Benign cluster	15	1	<b>6 (29)<sup>c</sup></b>						
Konstantinopoulos et al.		BRCA-like	32	0	2 (6)	0.7279 (-)		0.0043 (-)	7.6 × 10 <sup>-6</sup> (-)	0.34	0.19
		Non-BRCA-like	27	0	2 (7)						

Note: Details of published signatures are given in Supplementary Table S4A. **A**, Gene overlap between microdissected ovarian cancer gene signatures and both SGs and TGs of the AOCS microdissected data set. *P* values calculated with Fisher exact test. Association between gene signatures and the % stromal proportion (**B**) in TCGA ovarian cancer tumors or microdissected stroma in two breast cancer data sets (**C**) or two prostate cancer data sets (**D**). *P* values were calculated using linear regression (**B** and **D**) or *t* tests (**C**). Associations with stroma were mostly positive. Negative associations with stroma are indicated in parentheses (-) next to *P* values, and otherwise, associations were positive. No multiple testing correction was used.

<sup>a</sup>Total number of unique gene symbols reported in the specified gene signature from each study.

<sup>b</sup>*P* values derived using a paired *t* test or linear regression.

<sup>c</sup>*P* < 0.001.



## Stroma Impacts Cancer Subtype and Gene Signature Discovery

**Table 2.** Univariate and multivariate analysis of association between ovarian cancer gene signatures and OS of patients in (A) the TCGA data set (A) or the smaller MGH study (B).

Published gene signature		(A) HGSOc tumors (TCGA, <i>n</i> = 518) <sup>b</sup>				(B) MGH data ( <i>n</i> = 38)	
Study	Signature or % stromal content	OS	<sup>b</sup> OS, adjusted stage	<sup>b</sup> OS, adjusted % stroma	<sup>b</sup> OS, adjusted % stroma + stage	OS, gene expression in microdissected epithelium	OS, gene expression in microdissected stroma
AOCS C1 stroma vs. tumor <sup>a</sup>	Stromal genes vs. tumor genes	0.0870	0.137	0.2730	0.484	0.2440	0.1800
MGH stroma vs. tumor <sup>a</sup>	Tumor-associated stroma vs. tumor	<b>0.0336</b>	0.0544	0.148	0.289	0.555	0.156
MGH tissue-specific genes <sup>a</sup>	Tumor	0.778	0.640	0.996	0.906	0.924	0.718
	Tumor-associated stroma	<b>0.0430</b>	0.0732	0.177	0.337	0.540	0.164
	Normal or tumor-associated stroma	<b>0.0395</b>	0.0707	0.140	0.294	0.598	0.175
TCGA stromal content	Pathologist assessment of % stroma in TCGA samples	0.0979	<b>0.0499</b>	N/A	N/A	N/A	N/A
AOCS (Tothill et al.)	C1	<b>0.0175</b>	0.0658	0.0755	0.276	0.343	0.316
	PFS	<b>0.0045</b>	<b>0.0195</b>	<b>0.0346</b>	0.148	0.242	0.377
	OS	<b>0.0010</b>	<b>0.0068</b>	<b>0.0076</b>	0.0541	0.356	0.105
Bentink et al.	Angiogenic vs. nonangiogenic	<b>0.0313</b>	0.115	0.109	0.374	0.552	0.324
Bignotti et al.	Metastasis vs. primary	<b>0.0165</b>	0.0921	0.0613	0.311	0.383	0.229
Spentzos et al.	Prognosis	<b>0.0118</b>	<b>0.0330</b>	0.0507	0.163	0.608	0.145
Bonome et al.	Prognosis	<b>0.0426</b>	0.0571	0.128	0.208	0.366	<b>0.0352</b>
Biade et al.	Malignant vs. benign	0.310	0.266	0.587	0.584	0.642	0.101
Konstanti-nopoulos et al.	BRCA-like	<b>0.0167</b>	<b>0.0281</b>	<b>0.0272</b>	<b>0.0386</b>	0.696	0.387

Note: **A** and **B**, *P* values of Cox proportional hazard regression analysis. Significance (*P* < 0.05) is highlighted in bold.

<sup>a</sup>Supplementary Table S2.

<sup>b</sup>Multivariate survival analyses of TCGA data adjusted for percent stromal content and/or stage.

show that stromal genes differentiate the AOCS C1 molecular subtype or the TCGA mesenchymal subtype from other HGSOc molecular subtypes. This finding is supported by a recent IHC study of TCGA mesenchymal subtype tumors showing that several subtype marker genes were expressed exclusively or primarily in stroma (40). The dependence of the C1 subtype classifier on stromal genes may also explain why the TCGA mesenchymal subtype lacks robustness when applied to other data sets that may have variable tumor purity (8) and why few reproducible mutations or copy-number alternations have been described for the subtype. In miRNA analysis, the mesenchymal TCGA molecular subtype clusters with the proliferative subtype (2). In contrast, the AOCS C5 and TCGA proliferative subtypes are reported to have genetic alterations, including copy-number variation, in several genes (2, 34), and consistently, these subtypes' gene-expression patterns were not well explained by stromal genes.

Small increases in stromal gene expression caused subtype misclassification in our computational model that mixed stroma and tumor gene expression profiles. The influence of non-cancer cell gene expression on subtype classification is potentially a source of systematic error in other solid tumors. The accuracy of signature classifiers that predict breast tumor molecular subtype (PAM50) or risk of recurrence (Oncotype DX) decreases considerably with decreasing proportion of tumor cells and increasing proportion of normal cells (33). Molecular subtype definitions developed from gene-expression profiles of bulk ovarian, breast, and other carcinomas may need to be redefined such that molecular subtypes more precisely model the contributions of tumor, stroma, and other cell types. Thus far, at least two HGSOc

stroma subtypes have been proposed (16) and their relationships to epithelial HGSOc molecular subtypes are yet to be described.

Deconvolution of cell mixtures in bulk gene-expression studies is an active area of research (41), and we identified tissue-specific marker genes of HGSOc epithelial carcinoma and stroma (Supplementary Table S2) that may be applied to computational prediction of cell proportions and in the study of tumor/stroma interactions. These tissue-specific genes highlight the importance of studying both epithelial and stromal cell biology in cancer. *CEP55* had the highest specificity and sensitivity of the tumor-specific genes, and it codes for a protein that interacts with BRCA2 and plays a critical role in regulating the final step of cytokinesis (42). Some stroma-specific were possibly related either to macrophage activity or to the recently described TGFβ-dependent and TGFβ-independent Smad signaling (16) in stroma of HGSOc. Two of the 11 stroma-specific genes (*IFFO1* and *GLIPR1*) were strong predictors both of pathologist's stroma proportion scores in TCGA tumors (Pearson correlation 0.7 and 0.67, respectively, *P* < 0.0001) and of a gene signature that predicts macrophage/monocyte activity (Supplementary Fig. S4, colony-stimulating factor-1, CSF1 signature; refs. 17, 43). Three other stroma-specific genes were strongly correlated with TGCA immune landscape scores for TGFβ response (Supplementary Fig. S4) in TCGA tumors (17). These included thrombospondin 1 (*THBS1*), which is associated with tumor growth and metastasis in gastric carcinoma (44), and biglycan (*BGN*), which has been shown to form a complex with either TGFβ<sub>1</sub> or TGFβ<sub>1</sub> type I receptor to intensify the phosphorylation of Smad2/3 in cultured endothelial cells (45).

Further understanding of stromal cell biology in HGSOC would be valuable, particularly because stromal gene expression was associated with a worse prognosis (Table 2; ref. 12). Few studies provide pathologist estimates of stroma proportion, and we developed gene signature models for stroma proportion, which were weakly associated with worse survival in a meta-analysis of 2,527 tumors (HR 1.17; ref. 20). We performed a systematic analysis of published prognostic signatures in HGSOC and discovered that most, including the BRCA-ness signature (35), do not predict stroma proportion. Several signatures were highly enriched in stromal genes and did not provide additional prognostic information beyond the stromal cell proportion, suggesting that adjusting for stromal proportions may be useful in subtype and signature discovery.

In ovarian cancer, the link between stroma and survival may sometimes be related to other variables, such as the sampling methods. For example, the prognostic performance of the AOCs stroma-associated subtype, C1, is partly explained by stage or sampling location. This association with sampling location also suggests that stromal content may be variable within a single tumor or between studies. In Biade and colleagues (36), the benign rather than poor-prognosis tumors were enriched in stroma, and a recent analysis of tumor purity across several cancers showed that tumor purity's relationship with survival is often confounded with other variables (46).

These issues of sampling heterogeneity in bulk tissue were recognized as early as 1999 when Golub and colleagues (47) remarked: "Studies will require careful experimental design to avoid potential experimental artifacts – especially in the case of solid tumors. Biopsy specimens, for example, might have gross differences in the proportion of stromal cells. Furthermore, accumulating evidence suggests that the composition and gene expression of stroma may vary depending upon the specific anatomic location of the specimens. Blind application of class discovery could result in identifying classes reflecting the proportion of stromal contamination in the samples, rather than underlying tumor biology. Such 'classes' would be real and reproducible but would not be of biological or clinical interest."

Our results strongly support single-cell analysis or microdissection of tumor samples in gene-expression studies so that the features of the epithelial tumor cells, stromal, and immune components can be each analyzed. Retrospective analysis of bulk gene-expression patterns in light of emerging single-cell sequencing data is needed to refine molecular subtypes in ovarian cancer and other carcinomas and enable

a more comprehensive search for molecular targets amenable to therapeutic intervention.

## Disclosure of Potential Conflicts of Interest

C.S. Mitsiades is an employee at Takeda, reports receiving honoraria for one-time consulting/advisory board from Ionis Pharmaceuticals and Fate Therapeutics, and reports receiving commercial research grants from Janssen/Johnson & Johnson, TEVA, EMD Serono, AbbVie, Karyopharm, Sanofi, and Arch Oncology. W. Wei, G. Parmigiani, and M.J. Birrer have patent ownership in WO2014153442A2, METHODS AND SYSTEMS FOR TREATMENT OF OVARIAN CANCER. G. Parmigiani has ownership interest in CRA Health and Phaeno Biotech. J. Quackenbush is a scientific advisory board member for Caris Life Sciences. No potential conflicts of interest were disclosed by the other authors.

## Authors' Contributions

**Conception and design:** M. Schwede, S.C. Mok, J. Quackenbush, A.C. Culhane  
**Development of methodology:** M. Schwede, D.P. Harrington, A.C. Culhane  
**Acquisition of data (provided animals, acquired and managed patients, provided facilities, etc.):** M. Schwede, S.C. Mok, W. Wei, M.J. Birrer  
**Analysis and interpretation of data (e.g., statistical analysis, biostatistics, computational analysis):** M. Schwede, A. Basunia, G. Parmigiani, D.P. Harrington, M.J. Birrer, A.C. Culhane  
**Writing, review, and/or revision of the manuscript:** M. Schwede, L. Waldron, A. Basunia, M.A. Merritt, G. Parmigiani, D.P. Harrington, J. Quackenbush, M.J. Birrer, A.C. Culhane  
**Administrative, technical, or material support (i.e., reporting or organizing data, constructing databases):** M.J. Birrer, A.C. Culhane  
**Study supervision:** J. Quackenbush, M.J. Birrer, A.C. Culhane

## Acknowledgments

This study was supported in part by grants from the NCI at the NIH (RC4CA156551 to M.J. Birrer, P30CA006516 and R01CA174206 to G. Parmigiani, R01CA133057 to S.C. Mok, R03CA191447 to L. Waldron, U19CA148065 and P01CA087969 to J. Quackenbush) and the National Institute on Minority Health and Health Disparities at the NIH (G12MD007599 to L. Waldron) and by the Assistant Secretary of Defense Health Program, through the Breast Cancer Research Program (W81XWH-15-1-0013 to A.C. Culhane). Opinions, interpretations, conclusions, and recommendations are those of the authors and are not necessarily endorsed by the U.S. Department of Defense.

The costs of publication of this article were defrayed in part by the payment of page charges. This article must therefore be hereby marked *advertisement* in accordance with 18 U.S.C. Section 1734 solely to indicate this fact.

Received December 19, 2018; revised April 26, 2019; accepted December 6, 2019; published first December 23, 2019.

## References

- Tothill RW, Tinker AV, George J, Brown R, Fox SB, Lade S, et al. Novel molecular subtypes of serous and endometrioid ovarian cancer linked to clinical outcome. *Clin Cancer Res* 2008;14:5198–208.
- Cancer Genome Atlas Research Network. Integrated genomic analyses of ovarian carcinoma. *Nature* 2011;474:609–15.
- Waldron L, Haibe-Kains B, Culhane AC, Riester M, Ding J, Wang XV, et al. Comparative meta-analysis of prognostic gene signatures for late-stage ovarian cancer. *J Natl Cancer Inst* 2014;106. doi: 10.1093/jnci/dju049.
- Riester M, Wei W, Waldron L, Culhane AC, Trippa L, Oliva E, et al. Risk prediction for late-stage ovarian cancer by meta-analysis of 1525 patient samples. *J Natl Cancer Inst* 2014;106. doi: 10.1093/jnci/dju048.
- Waldron L, Riester M, Birrer M. Molecular subtypes of high-grade serous ovarian cancer: the holy grail? *J Natl Cancer Inst* 2014;106. doi: 10.1093/jnci/dju297.
- Konecny GE, Wang C, Hamidi H, Winterhoff B, Kalli KR, Dering J, et al. Prognostic and therapeutic relevance of molecular subtypes in high-grade serous ovarian cancer. *J Natl Cancer Inst* 2014;106. doi: 10.1093/jnci/dju249.
- Verhaak RGW, Tamayo P, Yang JY, Hubbard D, Zhang H, Creighton CJ, et al. Prognostically relevant gene signatures of high-grade serous ovarian carcinoma. *J Clin Invest* 2013;123:517–25.
- Chen GM, Kannan L, Geistlinger L, Kofia V, Safikhani Z, Gendoo DMA, et al. Consensus on molecular subtypes of high-grade serous ovarian carcinoma. *Clin Cancer Res* 2018;24:5037–47.
- Wang Y, Xia X-Q, Jia Z, Sawyers A, Yao H, Wang-Rodriguez J, et al. In silico estimates of tissue components in surgical samples based on expression profiling data. *Cancer Res* 2010;70:6448–55.
- Downey CL, Simpkins SA, White J, Holliday DL, Jones JL, Jordan LB, et al. The prognostic significance of tumour-stroma ratio in oestrogen receptor-positive breast cancer. *Br J Cancer* 2014;110:1744–7.
- Huijbers A, Tollenaar RA, v Pelt GW, Zeestraten EC, Dutton S, McConkey CC, et al. The proportion of tumor-stroma as a strong prognosticator for stage II and III colon cancer patients: validation in the VICTOR trial. *Ann Oncol* 2013;24:179–85.
- Chen Y, Zhang L, Liu W, Liu X. Prognostic significance of the tumor-stroma ratio in epithelial ovarian cancer. *BioMed Res Int* 2015;2015:589301.
- Joyce JA, Pollard JW. Microenvironmental regulation of metastasis. *Nat Rev Cancer* 2009;9:239–52.
- Bentink S, Haibe-Kains B, Risch T, Fan J-B, Hirsch MS, Holton K, et al. Angiogenic mRNA and microRNA gene expression signature predicts a novel subtype of serous ovarian cancer. *PLoS One* 2012;7:e30269.

## Stroma Impacts Cancer Subtype and Gene Signature Discovery

15. Zhang S, Jing Y, Zhang M, Zhang Z, Ma P, Peng H, et al. Stroma-associated master regulators of molecular subtypes predict patient prognosis in ovarian cancer. *Sci Rep* 2015;5:16066.
16. Yeung TL, Sheng J, Leung CS, Li F, Kim J, Ho SY, et al. Systematic identification of druggable epithelial-stromal crosstalk signaling networks in ovarian cancer. *J Natl Cancer Inst* 2018;111:272–82.
17. Thorsson V, Gibbs DL, Brown SD, Wolf D, Bortone DS, Ou Yang TH, et al. The immune landscape of cancer. *Immunity* 2018;48:812–30.
18. Mok SC, Bonome T, Vathipadiekal V, Bell A, Johnson ME, Wong K, et al. A gene signature predictive for outcome in advanced ovarian cancer identifies a survival factor: microfibril-associated glycoprotein 2. *Cancer Cell* 2009;16:521–32.
19. Leung CS, Yeung TL, Yip KP, Pradeep S, Balasubramanian L, Liu J, et al. Calcium-dependent FAK/CREB/TNNC1 signalling mediates the effect of stromal MFAP5 on ovarian cancer metastatic potential. *Nat Commun* 2014;5:5092.
20. Ganzfried BF, Riester M, Haibe-Kains B, Risch T, Tyekucheva S, Jazic I, et al. curatedOvarianData: clinically annotated data for the ovarian cancer transcriptome. *Database (Oxford)* 2013;2013:bat013.
21. Boersma BJ, Reimers M, Yi M, Ludwig JA, Luke BT, Stephens RM, et al. A stromal gene signature associated with inflammatory breast cancer. *Int J Cancer* 2008;122:1324–32.
22. Casey T, Bond J, Tighe S, Hunter T, Lintault L, Patel O, et al. Molecular signatures suggest a major role for stromal cells in development of invasive breast cancer. *Breast Cancer Res Treat* 2009;114:47–62.
23. McCall MN, Bolstad BM, Irizarry RA. Frozen robust multiarray analysis (fRMA). *Biostatistics* 2010;11:242–53.
24. Irizarry RA, Hobbs B, Collin F, Beazer-Barclay YD, Antonellis KJ, Scherf U, et al. Exploration, normalization, and summaries of high density oligonucleotide array probe level data. *Biostatistics* 2003;4:249–64.
25. Irizarry RA, Bolstad BM, Collin F, Cope LM, Hobbs B, Speed TP. Summaries of Affymetrix GeneChip probe level data. *Nucleic Acids Res* 2003;31:e15.
26. Benjamini Y, Hochberg Y. Controlling the false discovery rate: a practical and powerful approach to multiple testing. *J R Stat Soc Ser B Methodol* 1995;57:289–300.
27. Smyth GK. Linear models and empirical bayes methods for assessing differential expression in microarray experiments. *Stat Appl Genet Mol Biol* 2004;3:Article3.
28. Culhane AC, Thioulouse J, Perrière G, Higgins DG. MADE4: an R package for multivariate analysis of gene expression data. *Bioinformatics* 2005;21:2789–90.
29. McCall MN, Uppal K, Jaffee HA, Zilliox MJ, Irizarry RA. The gene expression barcode: leveraging public data repositories to begin cataloging the human and murine transcriptomes. *Nucleic Acids Res* 2011;39:D1011–5.
30. Sotiropoulos C, Wirapati P, Loi S, Harris A, Fox S, Smeds J, et al. Gene expression profiling in breast cancer: understanding the molecular basis of histologic grade to improve prognosis. *J Natl Cancer Inst* 2006;98:262–72.
31. Culhane AC, Schröder MS, Sultana R, Picard SC, Martinelli EN, Kelly C, et al. GeneSigDB: a manually curated database and resource for analysis of gene expression signatures. *Nucleic Acids Res* 2012;40:D1060–6.
32. Haibe-Kains B, Desmedt C, Loi S, Culhane AC, Bontempi G, Quackenbush J, et al. A three-gene model to robustly identify breast cancer molecular subtypes. *J Natl Cancer Inst* 2012;104:311–25.
33. Elloumi F, Hu Z, Li Y, Parker JS, Gulley ML, Amos KD, et al. Systematic bias in genomic classification due to contaminating non-neoplastic tissue in breast tumor samples. *BMC Med Genomics* 2011;4:54.
34. Helland Å, Anglesio MS, George J, Cowin PA, Johnstone CN, House CM, et al. Deregulation of MYCN, LIN28B and LET7 in a molecular subtype of aggressive high-grade serous ovarian cancers. *PLoS One* 2011;6:e18064.
35. Konstantinopoulos PA, Spentzos D, Karlan BY, Taniguchi T, Fountzilas E, Francoeur N, et al. Gene expression profile of BRCAness that correlates with responsiveness to chemotherapy and with outcome in patients with epithelial ovarian cancer. *J Clin Oncol* 2010;28:3555–61.
36. Biade S, Marinucci M, Schick J, Roberts D, Workman G, Sage EH, et al. Gene expression profiling of human ovarian tumours. *Br J Cancer* 2006;95:1092–100.
37. Bignotti E, Tassi RA, Calza S, Ravaggi A, Bandiera E, Rossi E, et al. Gene expression profile of ovarian serous papillary carcinomas: identification of metastasis-associated genes. *Am J Obstet Gynecol* 2007;196:245.
38. Bonome T, Levine DA, Shih J, Randonovich M, Pise-Masison CA, Bogomolny F, et al. A gene signature predicting for survival in suboptimally debulked patients with ovarian cancer. *Cancer Res* 2008;68:5478–86.
39. Spentzos D, Levine DA, Ramoni MF, Joseph M, Gu X, Boyd J, et al. Gene expression signature with independent prognostic significance in epithelial ovarian cancer. *J Clin Oncol* 2004;22:4700–10.
40. Zhang Q, Wang C, Cliby WA. Cancer-associated stroma significantly contributes to the mesenchymal subtype signature of serous ovarian cancer. *Gynecol Oncol* 2019;152:368–74.
41. Yoshihara K, Shahmoradgoli M, Martinez E, Vegesna R, Kim H, Torres-Garcia W, et al. Inferring tumour purity and stromal and immune cell admixture from expression data. *Nat Commun* 2013;4:2612.
42. Mondal G, Rowley M, Guidugli L, Wu J, Pankratz VS, Couch FJ. BRCA2 localization to the midbody by filamin A regulates cep55 signaling and completion of cytokinesis. *Dev Cell* 2012;23:137–52.
43. Beck AH, Espinosa I, Edris B, Li R, Montgomery K, Zhu S, et al. The macrophage colony stimulating factor-1 response signature in breast carcinoma. *Clin Cancer Res* 2009;15:778–87.
44. Lin XD, Chen SQ, Qi YL, Zhu JW, Tang Y, Lin JY. Overexpression of thrombospondin-1 in stromal myofibroblasts is associated with tumor growth and nodal metastasis in gastric carcinoma. *J Surg Oncol* 2012;106:94–100.
45. Hara T, Yoshida E, Shinkai Y, Yamamoto C, Fujiwara Y, Kumagai Y, et al. Biglycan intensifies ALK5-Smad2/3 signaling by TGF- $\beta$ 1 and downregulates syndecan-4 in cultured vascular endothelial cells. *J Cell Biochem* 2017;118:1087–96.
46. Aran D, Sirota M, Butte AJ. Systematic pan-cancer analysis of tumour purity. *Nat Commun* 2015;6:8971.
47. Golub TR, Slonim DK, Tamayo P, Huard C, Gaasenbeek M, Mesirov JP, et al. Molecular classification of cancer: class discovery and class prediction by gene expression monitoring. *Science* 1999;286:531–7.
48. Szklarczyk D, Franceschini A, Wyder S, Forslund K, Heller D, Huerta-Cepas J, et al. STRING v10: protein-protein interaction networks, integrated over the tree of life. *Nucleic Acids Res* 2015;43:D447–52.

# Cancer Epidemiology, Biomarkers & Prevention

## The Impact of Stroma Admixture on Molecular Subtypes and Prognostic Gene Signatures in Serous Ovarian Cancer

Matthew Schwede, Levi Waldron, Samuel C. Mok, et al.

*Cancer Epidemiol Biomarkers Prev* 2020;29:509-519. Published OnlineFirst December 23, 2019.

**Updated version** Access the most recent version of this article at:  
doi:[10.1158/1055-9965.EPI-18-1359](https://doi.org/10.1158/1055-9965.EPI-18-1359)

**Supplementary Material** Access the most recent supplemental material at:  
<http://cebp.aacrjournals.org/content/suppl/2019/12/21/1055-9965.EPI-18-1359.DC1>

**Cited articles** This article cites 43 articles, 8 of which you can access for free at:  
<http://cebp.aacrjournals.org/content/29/2/509.full#ref-list-1>

**Citing articles** This article has been cited by 3 HighWire-hosted articles. Access the articles at:  
<http://cebp.aacrjournals.org/content/29/2/509.full#related-urls>

**E-mail alerts** [Sign up to receive free email-alerts](#) related to this article or journal.

**Reprints and Subscriptions** To order reprints of this article or to subscribe to the journal, contact the AACR Publications Department at [pubs@aacr.org](mailto:pubs@aacr.org).

**Permissions** To request permission to re-use all or part of this article, use this link  
<http://cebp.aacrjournals.org/content/29/2/509>.  
Click on "Request Permissions" which will take you to the Copyright Clearance Center's (CCC) Rightslink site.